Numerical Modelling of Tri-axial Testing of Jointed Rocks using FLAC^{3D}

T. G. Sitharam*
Ravindra Dwivedi
Vidya Bhushan Maji

Department of Civil Engineering,
Indian Institute of Science,
Bangalore-560 012, India
**Email: sitharam@civil.iisc.ernet.in*

ABSTRACT

In this paper, numerical analysis of the jointed rock has been carried out to give better insight in to the mechanical behavior of discontinuities in rock masses. Intact rock mass has been discretized using three-dimensional cylindrical elements and the joints are explicitly modelled using three-dimensional gap and friction elements. The model is subjected to the uniform confining pressure on all sides and with uniform axial loading at the top. Elasto-plastic material behavior has been used in the analyses. The axial load is applied in series of steps or increments. The incremental solution is performed in step-by-step manner until the full specified load is applied. Numerical analysis has been carried out for two different rocks with single and multiple joints for different confining pressures. The inclination of discontinuity is varied from 0º to 90º with the major principal stress direction. Results have been presented in the form of stress-strain plots, failure stress versus joint inclination angle in the case of single joint and failure stress versus number of joints in case of multiple joints; the effect of co-efficient of friction along the plane of weakness is also studied in this paper. The results compare well with the experimental results. The major advantage of explicit modelling of discontinuities in three-dimension is that the mode of failure can be traced out and the detailed behavior of discontinuity can be studied in true three-dimensional state of stress.

Key words: Jointed rocks, finite element modelling, discontinuities, and interface element.

1. INTRODUCTION

In nature, rock exists as a discontinuous medium. It contains fissures, fractures, joints, bedding planes and faults with varying degree of strength along them. The study of mechanical behavior of discontinuities in rock engineering has posed several challenges to engineers because of difficulties involved in analyzing it. These discontinuities may exist with or without gouge material, and play a significant role in

controlling the strength and deformational characteristics of jointed rock mass. Modelling of these discontinuities in the rock mass to determine their influence on strength and deformation behavior of rock masses is very important for engineering design of civil structures in jointed rock mass. To understand the mechanical behavior of jointed rocks, three main approaches are generally used:

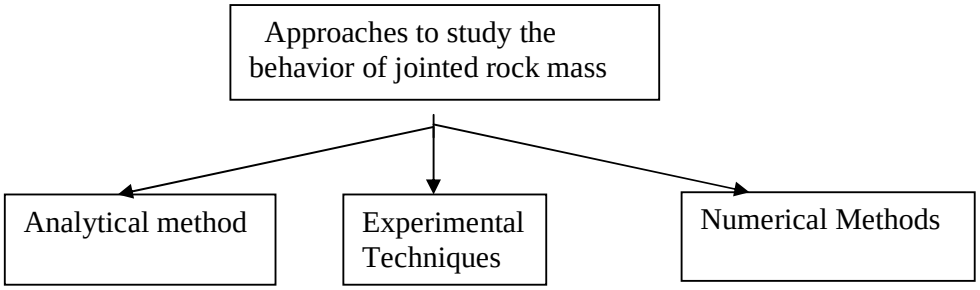

Analytical methods provide quick close form solutions, but they treat only simple geometries, and capture only the idealized structural theory. While using experimental techniques, representative or full-scale models can be tested. A number of experimental studies have been conducted both in-situ and in laboratory to understand the behavior of joints. Experimentation becomes time consuming and expensive, both in terms of the test facilities and instrumentation. Relative to analytical methods, numerical methods require very few restrictive assumptions and can treat complex geometries as well. They are far more cost effective than experimental techniques. Several numerical methods are available for modelling the jointed rock mass. All these numerical models have their own limitations and advantages. Numerical approaches considering explicit joints and as equivalent material for obtaining the overall response of jointed rock mass have been carried out in recent years (Goodman and Christopher, 1977; Pande et al., 1990; Ghaboussi et al., 1973; Zienkwicz et al., 1977; Desai et al., 1984; Gerrard, 1982; Pierce et al., 1992; Zhu and Wang, 1993; Crouch and Startfield, 1983; Lemos et al., 1985). Several numerical methods have been developed by various researchers to model the jointed rock mass using various techniques, e.g. finite element method, distinct element method and boundary element method.

In this paper, non-linear numerical analysis of the jointed rock mass has been carried out by representing the joints explicitly to study the mechanical behavior of discontinuities in the rock masses. Two different rock masses namely sandstone and granite have been analyzed with single and multiple joints for different joint inclination angles and confining pressures. The results have been presented in the form of stress-strain curves, failure stress versus number of joints, failure stress versus confining pressure, failure stress versus coefficient of friction, failure stress versus angle of inclination of joint with the major principal stress direction. The major advantage of explicit modelling of joints in the jointed rock mass is that the most probable failure pattern can be mapped from the equivalent plastic strain contours. The limitation of this method is that it is practically very difficult to model the rock masses with large number of joint sets. However, such an attempt to model the joints

explicitly will help in validating the futuristic "Practical Equivalent continuum" models (Sridevi et al., 1999; Sridevi and Sitharam, 1997, 2000; Sitharam et al., 2001; Sitharam and Madhavi Latha, 2002).

2. MODELLING DETAILS

Fast Lagrangian analysis of continua (FLAC) model (Itasca, 2000) has been used for the analyses. The jointed rock mass has been modelled using 3-dimensional cylindrical elements as shown in Fig.1 to represent the long body. Elasto-plastic material behavior with Mohr's yield criterion and perfectly plastic model with no strain softening is used in the analysis. In the case of elasto-plastic material behaviour, total deformation is composed of an elastic part and an elasto-plastic part. The elasto-plastic deformation starts when a specific combination of stress components, the equivalent stress, reaches the yield stress value. During the elasto-plastic deformation the yield stress will change as a function of the plastic strain.

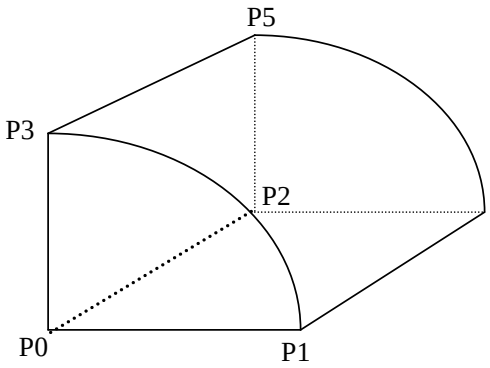

Fig. 1 – Cyllindrical element

In the present modelling, the type of material behavior is specified for each element of continuum. The non-linear elastic stress-strain curve is followed by each element up to the yield point, after which, the elements which have reached the yield point are showing elasto-plastic behavior. The non-linearity introduced due to change in the boundary at the joint is modelled explicitly using 3-dimensional triangular interface elements. Interface elements can be created at any location in space. These interface elements are attached to a zone surface face; two triangular interface elements are defined for every quadrilateral zone face. Interface nodes are then created automatically at every interface element vertex. When another grid surface comes into contact with an interface element, the contact is detected at the interface node and is characterized by normal and shear stiffness and sliding properties. Each interface element distributes its area to its nodes in a weighted fashion. Each interface node has an associated representative area. The entire interface is then divided into active interface, as shown in Fig. 2.

The fundamental contact relation is defined between the interface node and a zone surface face, also known as "target face". The normal direction of the interface face is

determined by target face. Interfaces are one sided in FLAC^{3D} as opposed to FLAC^{2D} in which interfaces are two sided.

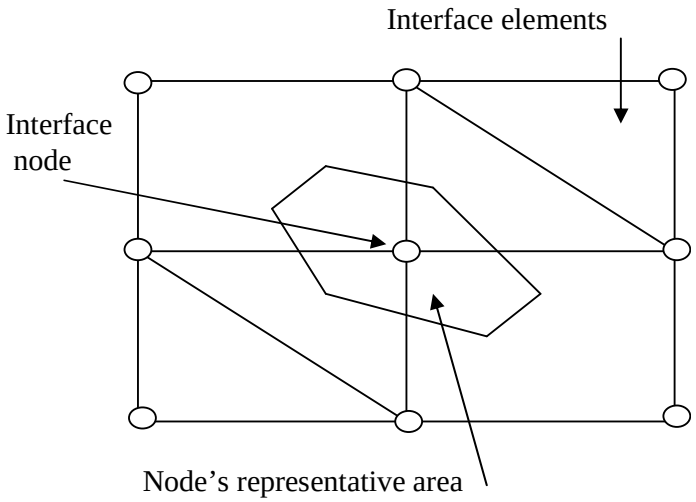

Fig. 2 – Distribution of representative areas to interface nodes

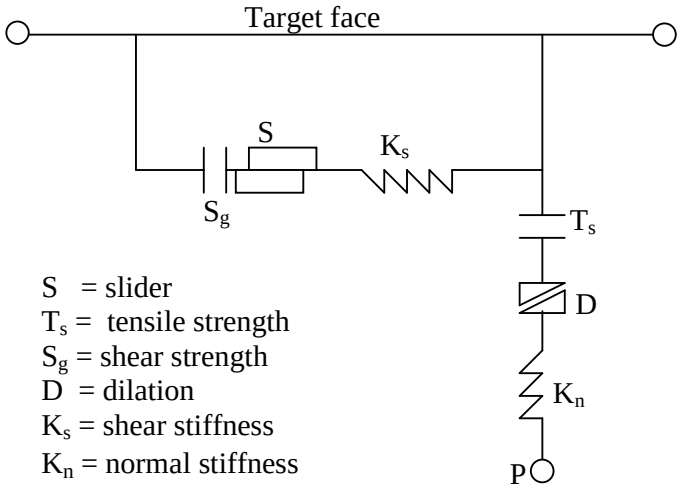

Fig. 3 - Components of the bonded interface constitutive model

During each time step, the absolute normal penetration and the relative shear velocity are calculated for each interface node and its contacting target face. Both of these values are used by the interface constitutive model to calculate absolute normal penetration and relative shear velocities. The constitutive model is defined by a non-linear elasto-plastic model using Mohr shear-strength criterion that limits the shear force acting at an interface node, normal and shears stiffnesses, tensile and shear bond strengths, and a dilation angle that causes an increase in effective normal force on the target face after the shear-strength limit is reached. Figure 3 shows the components of the constitutive model acting at the interface node (P).

The normal and shear forces that describe the elastic interface response are determined at calculation time (t + Δt) using the following relations.

$$F_n^{(t+\Delta t)} = k_n u_n A + \sigma_n A \quad (1)$$

$$F_{si}^{(t+\Delta t)} = F_{si}^{(t)} + k_s \Delta u_{si}^{(t+(0.5)\Delta t)} A + \sigma_{si} A \quad (2)$$

Where, $F_n^{(t+\Delta t)}$ is the normal force at time (t + Δt); $F_{si}^{(t+\Delta t)}$ is the shear force vector at time (t + Δt); u_n is the absolute normal penetration of the interface node into the target face; Δu_{si} is the incremental relative shear displacement vector; σ_n is the additional normal stress added due to interface stress initialization; k_n is the normal stiffness; k_s is the shear stiffness; σ_{si} is the additional shear stress vector due to interface stress initialization; and A is the representative area associated with the interface node. The inelastic interface logic works in the following way.

The Coulomb shear-strength criterion limits the shear force by the following relation.

$$F_{smax} = cA + \tan\varphi \, F_n \quad (3)$$

Where, *c* is the cohesion along the interface; φ is the friction angle [degrees] of the interface surface; and if the criterion is satisfied (if |Fs| ≥ Fsmax), then sliding is assumed to occur, and |Fs| = Fsmax, with the direction of shear force preserved. During sliding, shear displacement may cause an increase in the effective normal stress on the joint, according to the relation:

$$\sigma_n^{'} = \sigma_n + \frac{\left|F_s\right|_o - F_{s\max}}{Ak_s} \tan\Psi k_n \quad (4)$$

Where, $\sigma^{'}_n$ is increase in effective normal stress; ψ is the dilation angle [degrees] of the interface surface; and $|Fs|_o$ is the magnitude of shear force before the above correction is made.

3. NUMERICAL ANALYSIS

In the present analysis the jointed rock mass is modelled as shown in Figs. 4a and 4b. Single jointed rock (Fig. 4a) has single joint inclined at an angle β with the major principal stress direction. Multiple jointed rock (Fig. 4b) has 1, 2, 3 and 4 number of joints inclined at an angle β with the major principal stress direction. The intact rock elements are modelled using three-dimensional cylindrical elements as shown in Fig. 1 to represent the body of the jointed rock mass. Joints are modelled using 3-dimensional gap and friction elements. The interface elements are three-noded triangular interface elements used to model node to node contact between two bodies with and without friction. The model is subjected to the uniform confining pressure on all sides and followed by uniform axial stress on the top of the specimen.

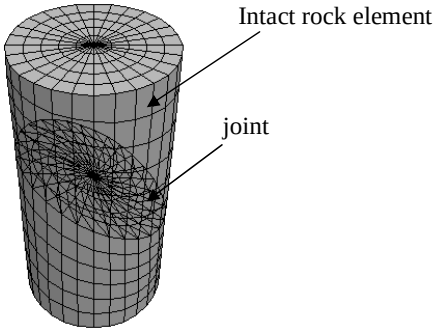

Fig. 4a – Single joint specimen (FLAC^{3D} model)

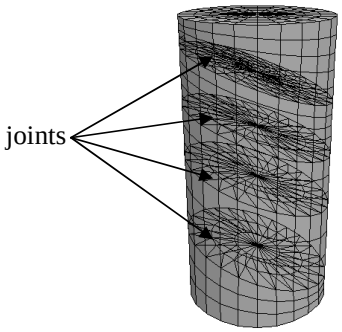

Fig. 4b – Multiple joint specimen (FLAC^{3D} model)

The non-linear static analysis is carried out with the assumptions that the material behavior is isotropic and homogenous and following elasto-plastic behavior with no strain softening. The axial load or deviator stress is applied (by controlling velocity) in series of steps or increments while the confining pressure applied on all the sides remains constant, till the specimen fails. The properties at the interface are derived from the definition of the interface elements and its function. The incremental analysis is preformed in a step-by-step manner until the full specified loads are applied. Mohr's yield criterion is used in the analysis to determine the major principal stress at failure.

For validation and study purpose, the numerical analysis has been carried out on the single and multiple jointed specimens of sandstone and granite. The intact rock properties used for the analyses are given in Table 1 (Yaji, 1984) and joint properties in Table 2.

Table 1 - Intact rock properties (Yaji, 1984)

Properties	Sandstone	Granite
Mass density (Kg/m^3)	2250	2650
Uni-axial compressive strength (MPa)	70	123
Cohesion (MPa)	13.0	25.5
Angle of Internal friction (°)	44.0	46.5
Elastic Modulus (GPa)	4.1	10.8
Classification	Hard rock	Extremely hard rock

Table 2 - Properties at the joint/interface (Assigned to the interface elements)

Property	For all the rock material at the interface
Axial stiffness in normal direction (K_n)	Four order magnitude times the stiffness of the adjacent elements (10^4)
Tangential stiffness (K_t)	1E-2 times K_n (10^{-2})

The results obtained have been compared with the available experimental results. The numerical results have been presented in the form of -

- Stress-Strain plot at different confining pressures
- Failure stress versus joint inclination for different confining pressure
- Failure stress versus coefficient of friction
- Failure stress versus number of joint
- Failure stress versus confining pressure
- Mode of failure and shear strain contours
- Comparison of FLAC2D and FLAC3D results

The stress corresponding to yield point is referred as failure stress. An element is observed to have failed when the yield criterion for the behavior is reached and the element behavior becomes plastic. The rock mass is found to have failed first in the region where the equivalent plastic strain occurs.

4. RESULTS

Results are grouped under the four following subheadings, as follows.

4.1 Single Jointed Rocks

In Figs. 5 a & 5b, deviator stress versus strain plot for granite and sandstone tri-axial samples have been presented with single joint orientation at 75° in case of granite sample and 60° in case of sandstone sample. Figures 5a and 5b also show the discretization adopted for single jointed specimen. In series of experiments, these single jointed specimen are subjected to different confining pressures (σ_3) of 1.0, 2.5, 5.0 MPa and additional deviatoric stress is applied. From the plots in Figs. 5a & 5b, it can be pointed out that the results predicted by FLAC^{3D} are much close to the experimental data (Yaji, 1984) in case of granite and similar results for sandstone at all the confining pressures. Plots also show that as the confining pressure is increasing the deviator stress is also increasing for the jointed rock mass.

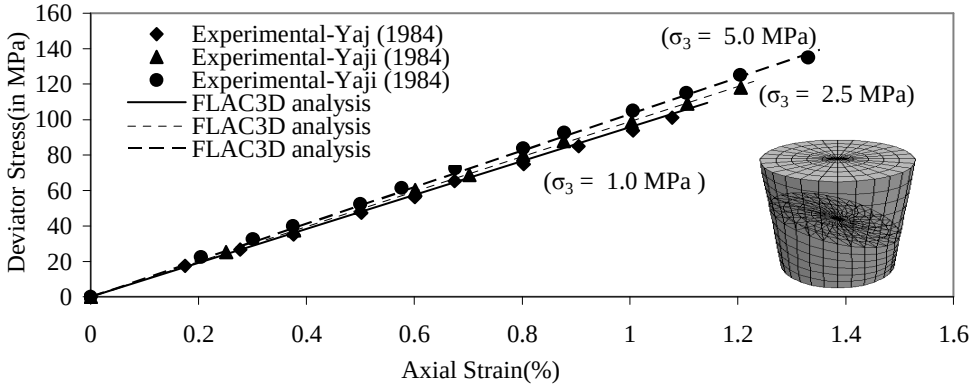

Fig. 5a – Stress-strain plot for granite (β = 75°) along with the experimental results (Yaji, 1984)

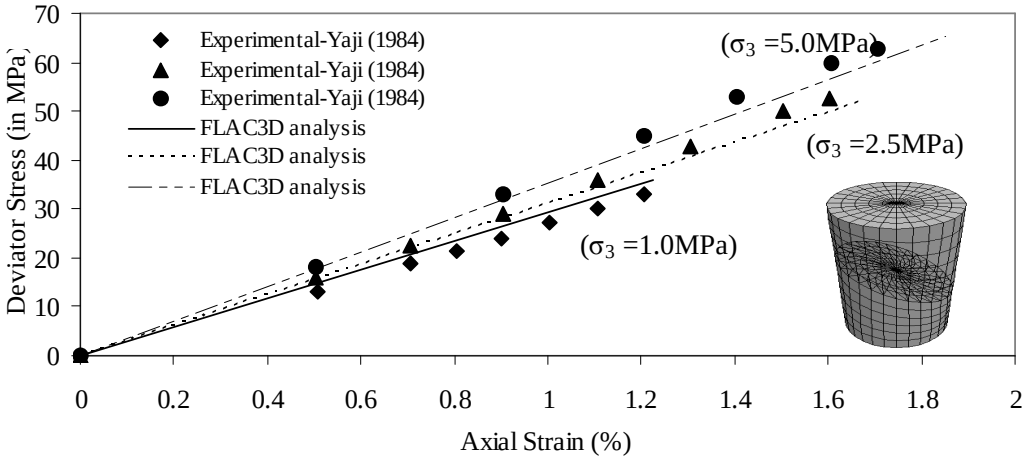

Fig. 5b – Stress-strain plot for sandstone (β = 60°) along with the experimental results (Yaji, 1984)

Figures 6a and 6b show the effect of angle of orientation of joint with the major principal stress direction for granite and sandstone rocks, respectively. From these plots, it can be pointed out that the failure stress is very small when the angle of inclination is in the range of 30º to 50º with the major principal stress direction and it is the maximum when the angle of inclination with the major principal stress is 0º and 90º, in both the cases. This is also true for the specimen subjected to the confining pressure of 2.5 and 5.0 MPa. Numerical results obtained using FLAC^{3D} are close to the experimental data (Yaji , 1984) as indicated in the Figs. 6a and 6b.

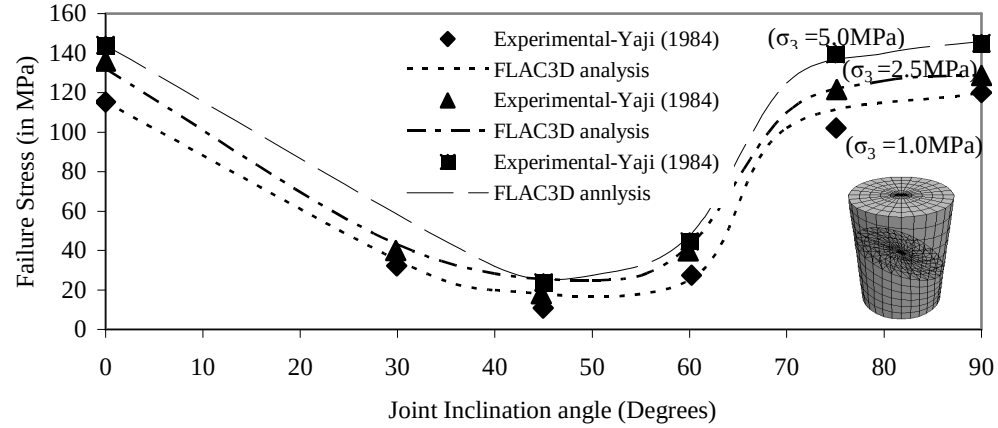

Fig. 6a – Failure stress plot for single jointed granite rock, experimental results (Yaji, 1984)

The study of coefficient of friction is very important, as surface roughness is perhaps the most important factor influencing the friction between joint surfaces, as it controls the movement along the joint planes. When a rock element slides over another, friction is mobilized along the contact surface. In Fig. 7, the effect of coefficient of friction along the plane of weakness has been analyzed and presented for granite and sandstone rock, respectively. From the plots, it can be pointed out that as the value of

coefficient of friction increases the resistance offered to slip increases till a certain value and further increase of coefficient of friction has no effect on the failure stress. Similar results have been presented by Sridevi et al. (2000) based on 2-dimensional non-linear FEM analysis.

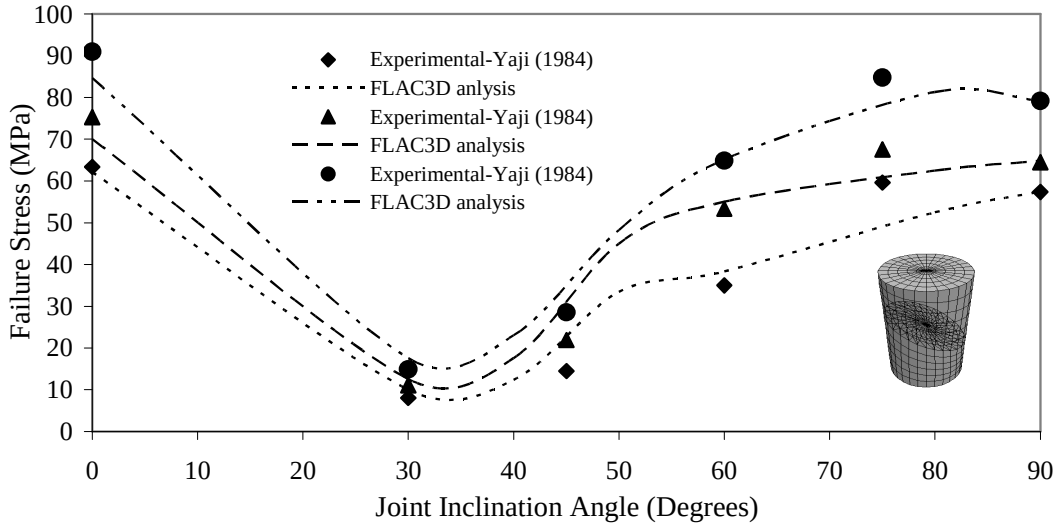

Fig. 6b – Failure stress plot for single jointed sandstone rock, experimental results (Yaji, 1984)

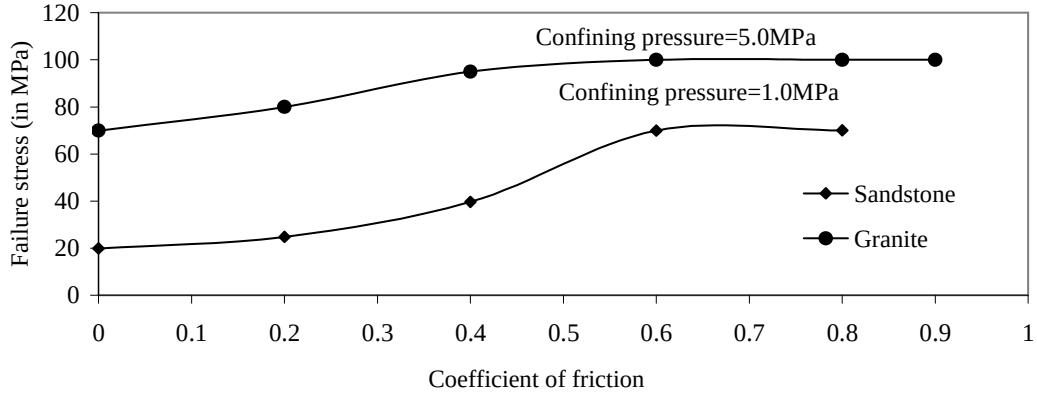

Fig. 7 – Variation of failure stress with coefficient of friction for single jointed specimen of granite ($\beta = 75°$) and sandstone ($\beta = 60°$)

4.2 Multiple Jointed Rocks

Multiple jointed specimen of sandstone and granite with different number of joints (such as 1, 2, 3, 4) subjected to different confining pressures, are analyzed. In Figs. 8a and 8b effects of confining pressure over jointed rock mass are presented. From the plots it may be pointed out that as the number of joints are increasing, the jointed rock mass failure stress decreases. Also, as the confining pressure increases jointed rock mass shear strength also increases, for both samples.

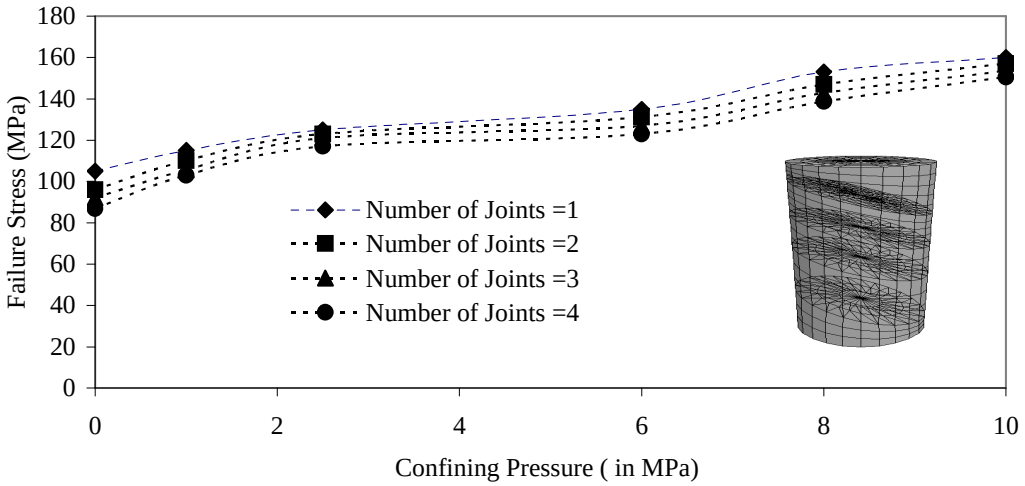

Fig. 8a - Effect of confining pressure on granite (β = 75°)

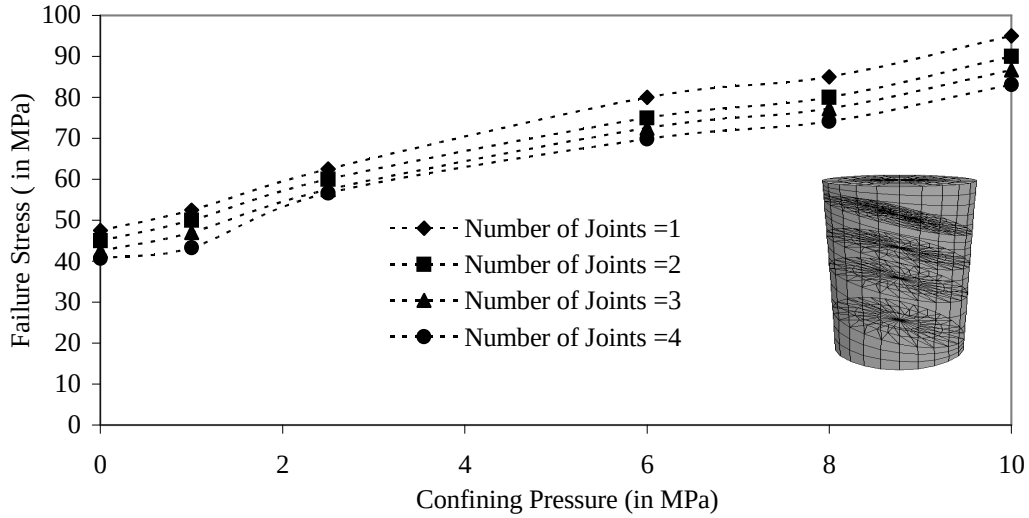

Fig. 8b – Effect of confining pressure on sandstone (β = 60°)

Figures 9a and 9b show the effect of number of joints over jointed rock mass failure stress. From the plots, it may be pointed out that as the number of joints is increasing; the failure stress of jointed rock mass decreases. The results compared well with the experimental results of Yaji (1984).

4.3 Mode of Failure

Figures 10a and 10b show shear strain rate and shear strain increment with the plane of failure for single jointed granite rock (β=75°) specimen. It is inferred from the plots that the jointed rock mass is failing along the plane of weakness.

Figures 11a and 11b show shear strain rate and shear strain increment with the plane of failure for sandstone single jointed (β=60°) specimen. In this case also similar results have been found out as from Figs. 10a & 10b.

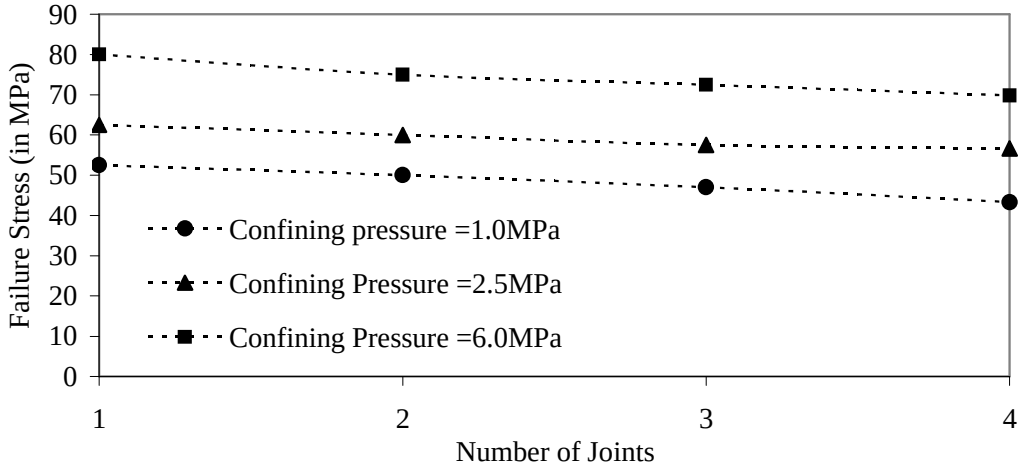

Fig. 9a – Failure stress plot for multiple jointed granite rock with different number of joints

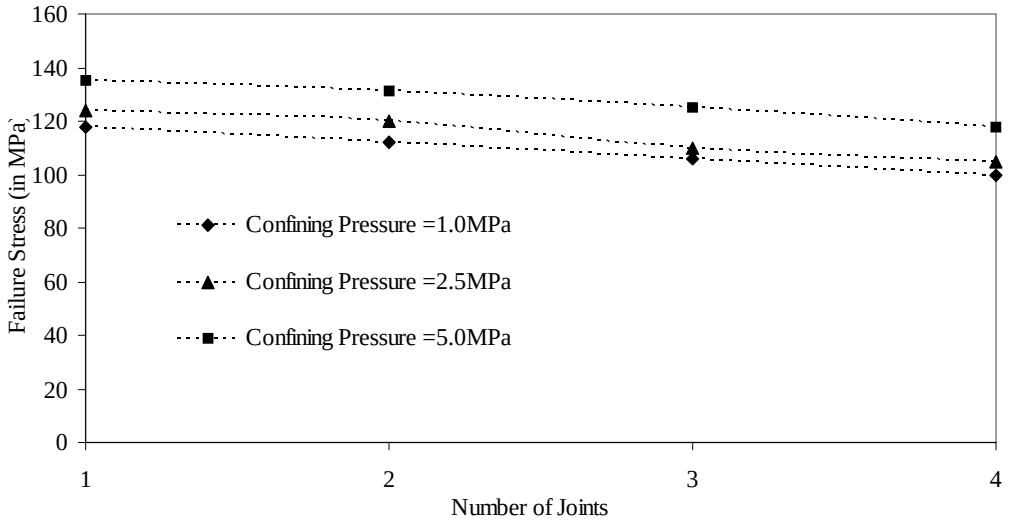

Fig. 9b – Failure stress plot for multiple jointed sandstone rock with different number of joints

4.4 Comparison of FLAC^{2D} and FLAC^{3D} Results

For the purpose of understanding the difference between FLAC^{2D} and FLAC^{3D} analyses, a comparative study has been done here. In the case of FLAC^{2D} analysis, the rock mass is discretized using 2-dimensional quadrilateral plane strain elements for representing long body and the non-linearity because of discontinuity has been modelled using 2-dimensional gap and friction interface elements. A uniform confining pressure is applied on all sides and followed by uniform axial loading at the top. Elasto-plastic material behavior with Mohr's yield criterion and perfectly plastic model with no strain softening is used in the analysis. The boundary conditions in this case are that the lower boundary is fixed in all the directions and the uniform confining pressure is applied on all the sides. At a given confining pressure the uniform axial loading has been applied by controlling the loading velocity; this is

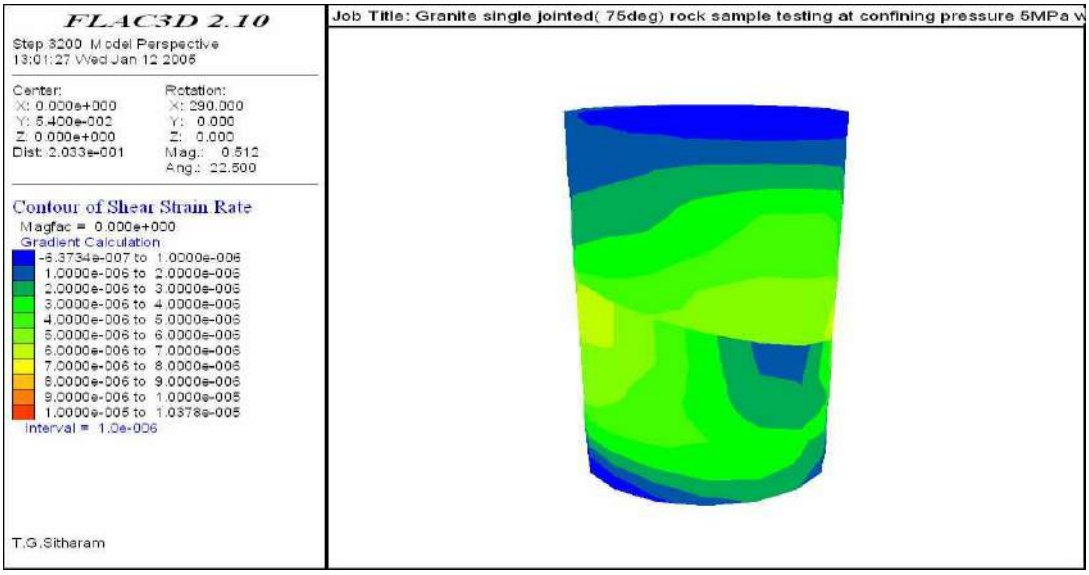

Fig. 10a - Shear strain rate contours

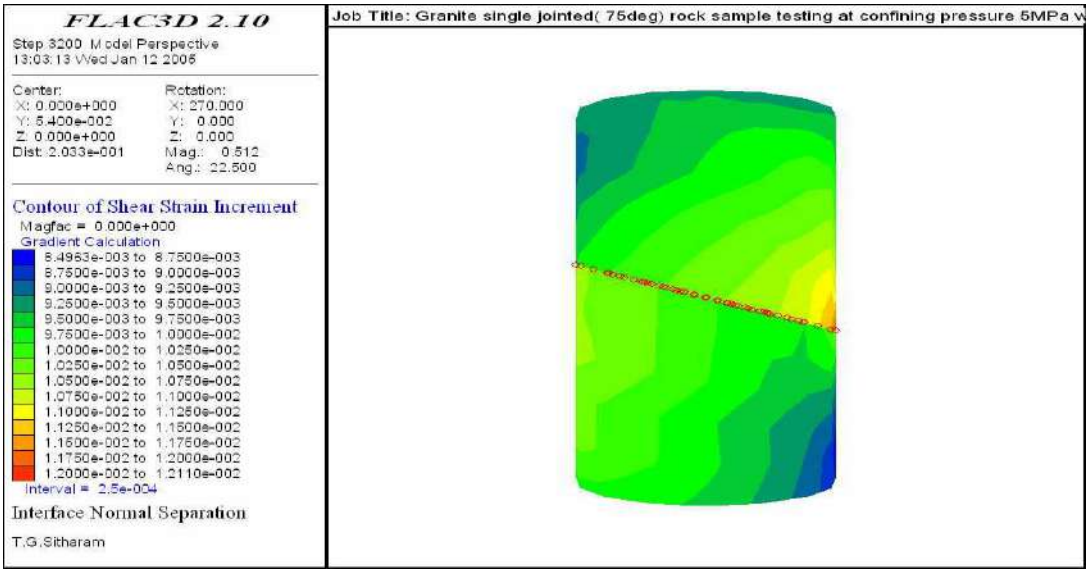

Fig. 10b - Shear strain increment contours with plane of separation

Fig. 10 - Mode of failure for single jointed Granite rock (β=75°) specimen

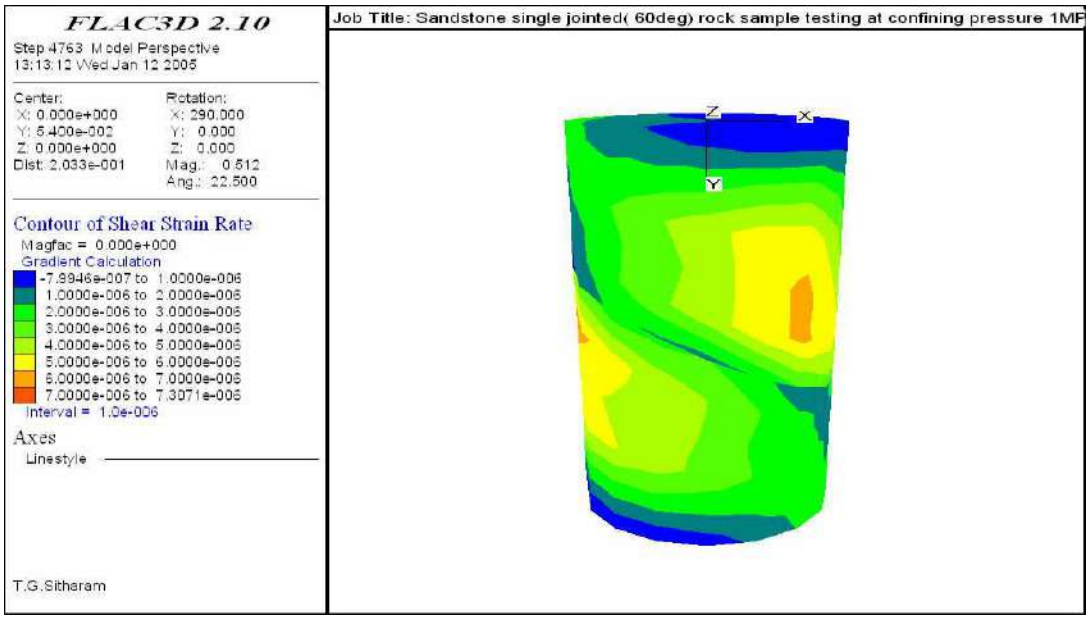

Fig.11a - Shear strain rate contours

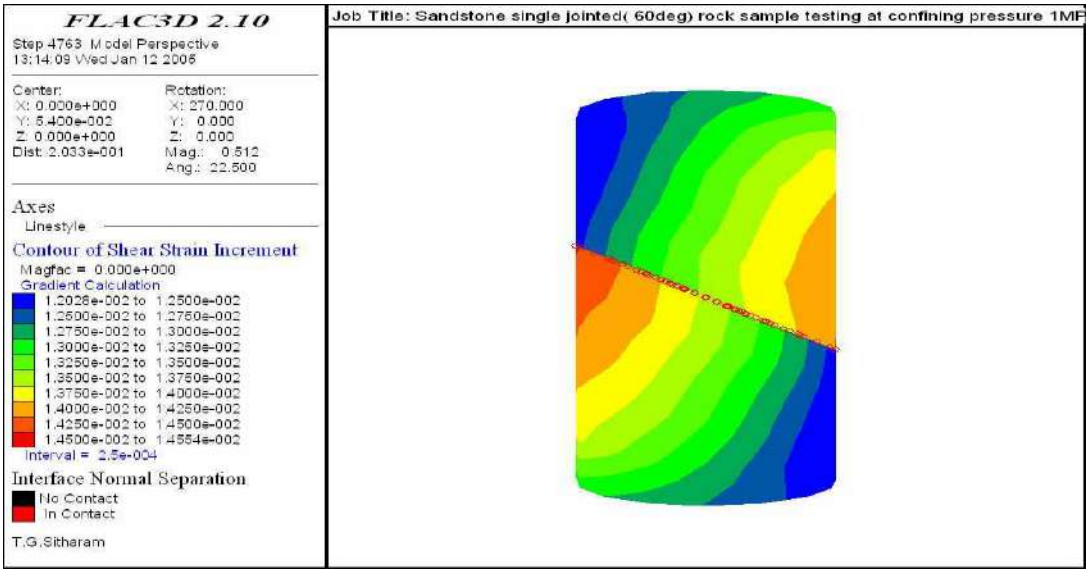

Fig. 11b - Shear strain increment contours with plane of separation

Fig. 11 - Mode of failure for single jointed Sandstone rock (β=60°) specimen

done by applying a small loading velocity. Figure 12 shows a typical comparison of FLAC^{2D} and FLAC^{3D} results. The results presented is for single jointed specimen of granite with β=75° at a confining pressure of 1.0 MPa. FLAC^{3D} results are closer to that of experimental results when compare to the results from FLAC^{2D}.

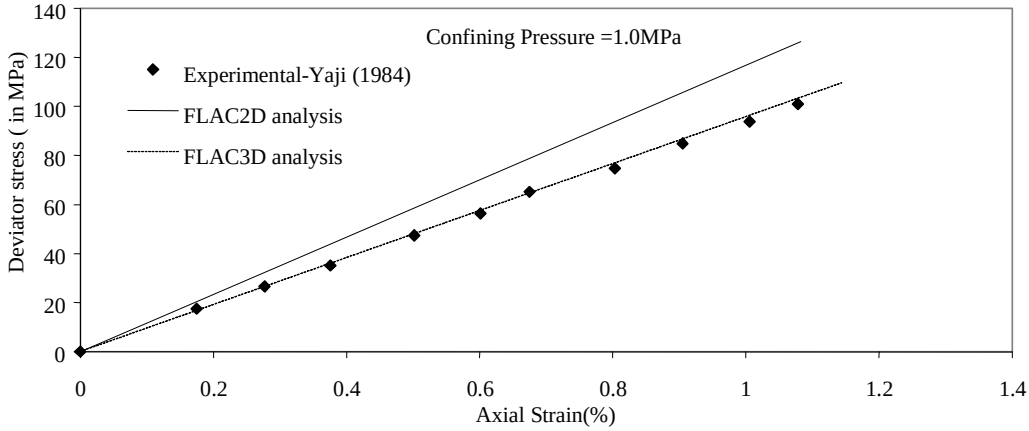

Fig. 12 – Comparison of FLAC2D and FLAC3D results with the experimental data for single jointed granite rock (β = 75°) (Yaji, 1984)

5. CONCLUSIONS

In this study the effects of (i) joint inclination angle, (ii) joint strength properties at the interface, (iii) confining pressure, and (iv) number of joints on the mechanical behaviour of jointed rock mass have been presented by carrying out a 3-dimensional analysis using FLAC^{3D}.

The results obtained from the numerical analysis using FLAC^{3D} match well with the experimental results. Following conclusions has been drawn from the study.

- It is clear from the results that the failure stress reaches a minimum value for joint inclination of 30º to 50º with the major principal stress direction, as expected.
- If the orientation of joint (single) is horizontal or vertical then the jointed rock mass is behaving as strong as intact rock.
- Joints weakens the rock mass and failure occurs at the interface when the joint inclination is 15º to 80º with the major principal stress direction, whereas the failure occurs in the intact rock when the inclination of joint is 0^o or 90º with the major principal stress direction.
- The number of joints present in the rock mass affect the strength and as the frequency of joints increases the strength of the rock mass comes down.
- The value of the coefficient of friction increases the resistance offered to slip and hence to failure at the interface.

The major advantages of explicit modelling of discontinuities are that the mode of failure can be traced out and the behavior of discontinuity can be mapped. Explicit modelling of joints using interface elements is suitable only for rocks having few major joints. This approach is not suitable to model highly discontinuous rocks as explicit modelling of a joint fabric is tedious and the analysis is highly complex and time consuming.

Acknowledgements

We thank Council of Scientific and Industrial Research (CSIR), Government of India, for the financial support under the project titled "Practical equivalent continuum modelling of jointed rocks and analysis of large-scale excavations in rock" (Ref. no. 70(0046)/03/EMR-II under extramural research division). This work has been carried out as part of this project.

References

Crouch, S. L. and Starfield, A.M. (1983). Boundary Element Methods in Solid Mechanics, ALLEN and Unwin London.

Desai, C.S. and Zaman, M.M. Lightner, J.G. and Siriwardane H.J. (1984). Thin-Layer Element for Interfaces and Joints, Int. J. Numer. Analy. Methods Geomech., Vol. 8, pp. 15-26.

Ghaboussi, J., Wilson, E. L. and Isenberg, J. (1973). Finite Element Analysis for Rock Joints and Interfaces, J. Soil Mech. Found. Div., American Soc. Civil Eng. 99, pp.833-848.

Gerrard, C.M. (1982). Equivalent Elastic Moduli of a Rock Mass Consisting of Orthorhombic Layers, Int. J. Rock Mech. Mining Sci. and Geomech. Abstr., Vol. 19, pp. 9-14.

Goodman, R.E. and Christopher, S.J. (1977). Finite Element Analysis for Discontinuous Rocks, Numerical Methods in Geotechnical Engineering, edited by C. S. Desai and J.T. Christain.

Itasca Consulting Group, Inc. Fast Lagrangian Analysis of Continua, FLAC (2000), Version 2.1.

Lemos, J.V., Hart, R.D. and Cundall, P.A. (1985). A Generalized Distinct Element Program for Modelling Jointed Rock Masses, Proc. Int. Symp on Fundamentals of Rock Joints, pp. 335-343.

Pande, G. N., Beer, G. and Williams, J.R. (1990). Numerical Methods in Rock Mechanics, pp. 98-102, Wiley, Chichester.

Peirce, A.P., Spottiswodde, S. and Napier, J.A.L. (1992). The Spectral Boundary Element Method: A New Window on Boundary Elements in Rock Mechanics, Int. J. Rock Mech. Min. Sci. & Geomech. Abstr. Vol. 29, No.4, pp.379-400.

Sitharam, T. G. and Sridevi, J. (1997). Non-linear Analysis of Jointed Rock using Equivalent Continuum Approach, Journal of Rock Mechanics and Tunnelling Technology, Vol. 3, No.2, pp.109-126

Sridevi, J. and Sitharam, T.G. (2000). Analysis of Strength and Modulli of Jointed Rocks, International Journal of Geotechnical and Geological Engg., Vol. 18, pp. 1-19.

Sitharam, T. G. and Madhavi Latha, G. (2002). Simulation of Excavations in Jointed Rock Masses using a Practical Equivalent Approach, Vol. 39, pp. 517-525.

Sitharam, T.G., Sridevi, J. and Shimizu, N. (2001). Practical Equivalent Continuum Characterization of Jointed Rock Masses, Vol. 38, pp. 437-448.

Sridevi, J., Sitharam, T.G. and Chandrashekar, H.M. (2000). Simulation of Jointed Rock Mass Behavior using Finite Element Method, Vol. 6, No. 2, pp.113-132.

Yaji, R. K. (1984). Shear Strength and Deformation of Jointed Rocks, Ph. D. Thesis, Indian Institute of Technology, Delhi, India.

Zienkiewicz, O.C., Kelly, D.W. and Bettess, P. (1977). The Coupling of the Finite Element Method and Boundary Solution Procedures. Int. Journal for Numerical Methods in Engineering, Vol.11, pp.355-375.

Zhu, W. and Wang, T. (1993). Finite Element Analysis of Jointed Rock Masses and Engineering Application, Int. J. Rock Mech. Min. Sci. & Geomech. Abstr., Vol. 30, No. 5, pp. 537-544.